EVIDENCE FOR ASYMMETRIC DISTRIBUTION OF CIRCUMSTELLAR MATERIAL AROUND TYPE Ia SUPERNOVAE

Francisco Förster[1], Santiago González-Gaitán[1], Joseph Anderson[1], Sebastián Marchi[1],
Claudia Gutiérrez[1], Mario Hamuy[1], Giuliano Pignata[2], and Régis Cartier[1]

[1] Departamento de Astronomía, Universidad de Chile, Casilla 36-D, Santiago, Chile
[2] Departamento Ciencias Físicas, Universidad Andres Bello, Av. República 252, Santiago, Chile

ABSTRACT

We study the properties of low-velocity material in the line of sight toward nearby Type Ia supernovae (SNe Ia) that have measured late phase nebular velocity shifts (v_{neb}), thought to be an environment-independent observable. We have found that the distribution of equivalent widths of narrow blended Na I D1 and D2 and Ca II H and K absorption lines differs significantly between those SNe Ia with negative and positive v_{neb}, with generally stronger absorption for SNe Ia with $v_{neb} \geqslant 0$. A similar result had been found previously for the distribution of colors of SNe Ia, which was interpreted as a dependence of the temperature of the ejecta with viewing angle. Our work suggests that (1) a significant part of these differences in color should be attributed to extinction, (2) this extinction is caused by an asymmetric distribution of circumstellar material (CSM), and (3) the CSM absorption is generally stronger on the side of the ejecta opposite to where the ignition occurs. Since it is difficult to explain (3) via any known physical processes that occur *before* explosion, we argue that the asymmetry of the CSM is originated *after* explosion by a stronger ionizing flux on the side of the ejecta where ignition occurs, probably due to a stronger shock breakout and/or more exposed radioactive material on one side of the ejecta. This result has important implications for both progenitor and explosion models.

Key words: distance scale – supernovae: general

Online-only material: color figures

1. INTRODUCTION

Type Ia supernovae (SNe Ia) are important tools for understanding the evolution of the universe because of their high luminosities and light curve homogeneity, which led to their standardization for cosmological distance measurements (Phillips 1993; Hamuy et al. 1996) and the discovery of the acceleration of the universe (Riess et al. 1998; Perlmutter et al. 1999). They are also important because of their complex nucleosynthetic output and high ejecta kinetic energies (10^{51} erg), which make them key ingredients for galaxy evolution theory.

Unfortunately, we still lack a clear understanding of the nature of SN Ia progenitors. Although it is generally accepted that their progenitors are carbon oxygen white dwarfs (CO WD) in mass transferring binary systems (for a review, see Hillebrandt & Niemeyer 2000), there is no agreement on what their companions are, whether the CO WD reaches the Chandrasekhar mass at ignition, what the mechanism that triggers the ignition is, and how the CO WD burns to form the ejecta.

Perhaps the two scenarios that best match observed SN Ia spectra and light curves are those considered in Röpke et al. (2012): either a stably accreting CO WD that reaches the Chandrasekhar mass (M_{Ch}), undergoes a thermonuclear runaway, and burns in a deflagration to detonation transition, in the M_{Ch}–single degenerate (SD) scenario (Nomoto et al. 1984; Khokhlov 1991); or a pair of CO WDs that merge and ignite dynamically in the violent double degenerate (DD) scenario (Pakmor et al. 2012).

Two significant differences between both scenarios are the typical central densities at ignition and the distribution of circumstellar material (CSM) around their progenitor systems. In the M_{Ch}–SD scenario, the central density at ignition is sufficiently high to avoid the synthesis of radioactive ^{56}Ni in

favor of stable iron group elements (IGEs) in the innermost regions of the ejecta. The M_{Ch}–SD scenario has potentially abundant CSM that could be produced by either the wind of the donor star, weak nova explosions experienced by the accretor, or by mass loss due to inefficient mass transfer. In the violent DD-scenario, conversely, the primary central density is never high enough to avoid the synthesis of radioactive ^{56}Ni in the innermost regions of the ejecta, and since the merger and ignition happen in a dynamical timescale, there is no time to leave a significant imprint in the CSM.

The M_{Ch}–SD scenario appears to overproduce IGEs (Nomoto et al. 1984), which are not produced significantly in the violent DD scenario. Observations of flat-topped profiles of Fe II lines in the optical and NIR at late phases have been argued to be evidence for stable IGEs in the innermost regions of the ejecta (Höflich et al. 2004; Gerardy et al. 2007). Moreover, significant nebular velocity shifts (v_{neb}) measured in these flat-topped profiles have been suggested as evidence for off-center ignition scenarios, which are expected in M_{Ch}–SD scenarios (see, e.g., Nonaka et al. 2012). The relation between v_{neb} and other properties such as the rate of evolution of the velocity of Si absorption lines (the *velocity gradient*) or the colors during the photospheric phase of evolution (Maeda et al. 2010, 2011; Cartier et al. 2011) seems to lend support to this picture.

For the nearby SN 2011fe, there is evidence for the lack of interaction between the ejecta and a companion star or a companion star wind. The radius of the companion star has been constrained to be less than 0.1 $R_\odot$ (Bloom et al. 2012; Nugent et al. 2011; Brown et al. 2012), and its mass loss, less than $\approx 10^{-8} M_\odot$ yr^{-1} (Horesh et al. 2012). However, Sternberg et al. (2011) showed that SNe Ia show an excess of blueshifted narrow Na lines, which is evidence for CSM around

type Ia progenitors ejected before explosion. Particular cases, specifically SN 2002ic (Hamuy et al. 2003), SN 2006X (Patat et al. 2007, cf. Chugai 2008), SN 1999cl (Blondin et al. 2009), and SN 2007le (Simon et al. 2009) have also provided evidence for CSM around SNe Ia, although in the case of SN 2002ic the nature of the explosion is unclear (Benetti et al. 2006).

Simon et al. (2009) noted that SNe Ia with variable narrow absorption lines tend to have broad lines and high velocity gradients. Foley (2012) recently suggested that higher velocity at peak, redder SNe Ia are preferentially found in lower mass host galaxies, but also that they have an excess of blueshifted absorption systems (Foley et al. 2012). These observations highlight the importance of understanding the relation between progenitor systems and dust properties for cosmological distance determinations (e.g., Goobar 2008; Folatelli et al. 2010). Since SNe Ia with $v_{neb} \geqslant 0$ are known to have higher velocity gradients, generally associated with higher velocities at peak, and to be redder (Maeda et al. 2010, 2011), we investigate the relation between the presence or absence of narrow Na I D1 and D2 and Ca II H and K absorption lines (hereafter Na and Ca lines), a proxy for material in the line of sight, with v_{neb}, a geometrical proxy that should depend only on viewing angle (Maeda et al. 2010) and that should therefore be independent of any evolutionary or host galaxy effects.

2. SAMPLE SELECTION AND DATA ANALYSIS

In this work, we have used the sample of 25 nearby SNe Ia with measured nebular velocity shifts (v_{neb}) derived by Blondin et al. (2012) and Maeda et al. (2011) for which we have measured equivalent widths (EWs) of Na (24 SNe) and Ca (23 SNe) absorption systems. The EWs were obtained from mid-resolution spectra in the public Center for Astrophysics (CfA) spectra database (Blondin et al. 2012; Jha et al. 1999; Branch et al. 2003; Matheson et al. 2008; Wang et al. 2009) for most SNe Ia; from Silverman et al. (2011) for SN2009dc; from high-resolution spectra in the European Southern Observatory (ESO) archive for SN 2000cx, SN 2001el, and SN 2006X; from Sternberg et al. (2011) for SN 2007sr and SN 2007af; using Yaron & Gal-Yam (2012); values from the literature for SN 1986G, SN 2004eo, and SN 2006dd (Phillips 1987; Pastorello et al. 2007; Stritzinger et al. 2010); and our own X-Shooter (Vernet et al. 2011) data for SN 2010ev. We note that although there are public spectra for SN 1990N and SN 2004eo, we do not use them because they appear to have been artificially smoothed in the wavelength direction, removing all evidence for narrow lines.

2.1. Equivalent Width Determination

We have written a Python script to measure EWs in every SN for every epoch available. The script first defines the continuum by tracing straight lines between nodes automatically defined. The position of the nodes is chosen to avoid being too close to the lines being measured, and the flux associated with every node is defined by locally averaging the observed flux with typical velocity ranges proportional to the separation between nodes and a continuous smoothing function. After the nodes are placed and the continuum defined, we visually inspect the spectra, divide the observed flux by the continuum, and compute the area below unity within 300 km s^{-1} of every line in Å:

$$\text{EW} = \sum_i \frac{\bar{f}_i - f_i}{\bar{f}_i} d\lambda = \sum_i \left(1 - \frac{f_i}{\bar{f}_i}\right) d\lambda, \qquad (1)$$

where f_i are the fluxes of pixels with velocities within 300 km s^{-1} of the line of interest, $\bar{f}_i$ is the continuum value for every pixel, and $d\lambda$ is the wavelength separation between pixels. In order to obtain more robust EW determinations, for every SN we use the median EW among all available epochs, excluding those epochs with significantly larger errors.

We have considered four sources of error in our method somewhat conservatively: flux measurement uncertainties (σ_f), continuum flux uncertainties (σ_c), possible systematic deviations in our method (σ_{sys}), and the median absolute deviation (a robust error measurement) of the EWs for different epochs for every SN (σ_{MAD}). σ_f and σ_c were obtained using the quoted flux uncertainties for every spectra at different wavelengths and propagating errors using Equation (1) to compute the EW uncertainty, σ_{EW}:

$$\sigma_{EW}^2 = \sum_i \left[\left(\frac{\sigma_{f_i}}{\bar{f}_i}\right)^2 + \left(\frac{f_i}{\bar{f}_i}\frac{\sigma_{\bar{f}_i}}{\bar{f}_i}\right)^2 \right] d\lambda^2 \equiv \sigma_f^2 + \sigma_c^2, \qquad (2)$$

where σ_{f_i} are the flux uncertainties in every pixel, $\sigma_{\bar{f}_i}$ is the uncertainty associated with the continuum at every pixel, defined as the average node flux uncertainty of the closest two nodes to every pixel, and where each node uncertainty is defined by weighting the σ_{f_i}'s in the same way as the flux of every node is defined.

To determine σ_{sys}, we have run our script assuming that the lines are in positions of the spectra where no low-velocity absorption lines should be found, changing these positions artificially along the spectra and using quadratically averaged values of the derived EWs as the final errors. To determine σ_{MAD}, we simply computed the median absolute deviation of the measured EWs at different epochs, excluding those values with relatively large errors.

2.2. Validation of the Method

We have compared our measurements of the EWs with those in the literature and with those obtained from publicly available high-resolution spectra, as shown in Figure 1. Our results are consistent within errors in 14 out of 15 measurements, with the only exception being SN 1998bu, for which we obtained a significantly higher EW, that upon visual inspection appears to be due to continuum definition uncertainties. We have also compared our measurements with those obtained with IRAF's *splot* routine and found consistent values in 90% of the cases, without any highly significant exception. The nebular velocities and EWs used in this analysis are shown in Table 1.

3. RESULTS

In order to test whether SNe Ia with negative and positive v_{neb} have different distributions of intervening material in the line of sight, we have performed Kolmogorov–Smirnov (K-S) tests of the cumulative distribution function (CDF) of the measured EWs of Na and Ca lines caused by intervening material in the Milky Way and in the SN host galaxies. We have also tested whether SNe Ia with negative or positive v_{neb} have different extinction or color properties using $E(B - V)$ values obtained with SNooPy (Burns et al. 2011) and $(B - V)_{B_{max}}$ values from SiFTO (Conley et al. 2008) best-fitting models. The K-S test results are shown in Table 2.

As expected, the distribution of intervening Milky Way material between SNe Ia with negative and positive v_{neb} is consistent with being drawn from the same parent population.
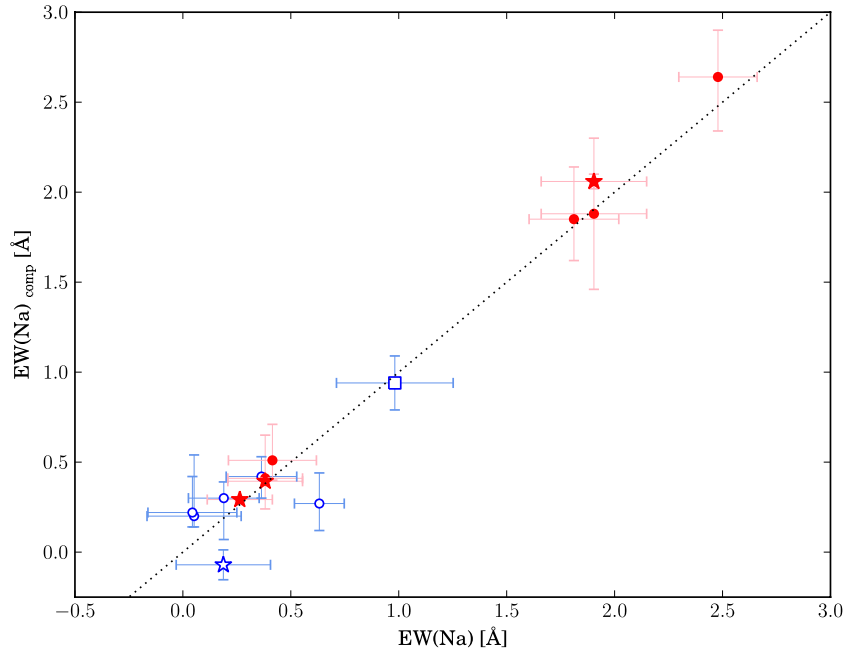
Figure 1. Comparison of measured equivalent widths of blended Na absorption features due to intervening material at the distance of the SNe Ia. We show the values obtained with our Python script using mid-resolution spectra, EW(Na), and compare them with those in Blondin et al. (2009), *circles*, Taubenberger et al. (2011), *square*, and high-resolution spectra measurements, *stars*. Red filled symbols are SNe Ia with $v_{neb} \geqslant 0$ and blue open symbols are SNe Ia with $v_{neb} < 0$. The dotted line shows the $EW(Na)_{comp} = EW(Na)$ relation. The only SN Ia with significantly different measurements in our sample is SN 1998bu, with $v_{neb} < 0$, and for which we measure a higher EW than Blondin et al. (2009).

(A color version of this figure is available in the online journal.)

Table 1
Supernovae with Available Nebular Velocities and Their Measured Equivalent Widths (EWs) for Na and Ca Lines in Å as Described in the Text

Name	v_{neb} (km s^{-1})	EW(Na)	EW(Ca)
SN 1986G	-639 ± 600	3.60 ± 0.01	1.75 ± 0.01
SN 1990N	-478 ± 600	NA	NA
SN 1994D	-2220 ± 220	0.05 ± 0.22	0.06 ± 0.25
SN 1994ae	-1204 ± 600	0.36 ± 0.16	0.33 ± 0.22
SN 1995D	-1193 ± 600	0.32 ± 0.21	0.23 ± 0.29
SN 1997bp	2539 ± 410	1.81 ± 0.21	1.12 ± 0.26
SN 1998aq	-1157 ± 129	0.19 ± 0.16	0.35 ± 0.20
SN 1998bu	-1351 ± 305	0.63 ± 0.12	0.07 ± 0.16
SN 2000cx	-172 ± 600	-0.07 ± 0.08	-0.01 ± 0.01
SN 2001el	980 ± 206	0.66 ± 0.04	0.67 ± 0.10
SN 2002bo	2258 ± 361	2.48 ± 0.18	1.20 ± 0.26
SN 2002dj	2021 ± 414	1.09 ± 0.33	0.78 ± 0.31
SN 2002er	582 ± 600	1.77 ± 0.17	1.62 ± 0.31
SN 2003du	-443 ± 283	0.07 ± 0.21	-0.02 ± 0.22
SN 2003hv	-2825 ± 384	-0.09 ± 0.25	-0.41 ± 0.41
SN 2003kf	1070 ± 201	0.41 ± 0.20	0.69 ± 0.25
SN 2004dt	-2623 ± 600	0.23 ± 0.23	-0.02 ± 0.36
SN 2004eo	-170 ± 25	0.00 ± 0.20	NA
SN 2005cf	-123 ± 600	0.04 ± 0.21	0.23 ± 0.20
SN 2006X	2832 ± 343	2.06 ± 0.04	0.80 ± 0.06
SN 2006dd	-1553 ± 201	3.22 ± 0.08	1.23 ± 0.21
SN 2007af	831 ± 350	0.39 ± 0.02	0.28 ± 0.17
SN 2007sr	1185 ± 600	0.29 ± 0.01	0.09 ± 0.26
SN 2009dc	-1190 ± 600	0.94 ± 0.15	2.00 ± 0.31
SN 2010ev	2145 ± 225	0.67 ± 0.05	0.37 ± 0.02

**Note.** NA indicates that data are not available.

However, the likelihood that the distribution of intervening material in their host galaxies is the same is significantly smaller. Given that the separation of the sample by the sign of v_{neb} should be purely geometrical, we should not expect any significant differences in the distributions of host Na and Ca lines, unless the intervening material is of a circumstellar nature and with an asymmetric distribution.

To test whether the different distributions of EWs are caused by an unlikely combination of host galaxy properties, we compare the distributions of host galaxy morphological types and inclinations from the Asiago catalog (Barbon et al. 1999) and the higher resolution normalized cumulative rank (NCR) pixel based statistic (James & Anderson 2006) that quantifies any association with regions of star formation (SF) using *Galaxy Evolution Explorer* (*GALEX*) NUV (23 out of 25 SNe) and our own Hα maps (14 out of 25 SNe), separating between SNe Ia with $v_{neb} \geqslant 0$ and $v_{neb} < 0$. We do not find any significant difference between these two populations for global (morphological type and inclination) or local (NCR statistics) host galaxy properties. The K-S test *p*-values are shown in Table 3.

In Figure 2, we plot the measured EWs for the Na and Ca lines divided by the sign of v_{neb}. Red filled symbols are SNe with $v_{neb} \geqslant 0$, and blue open symbols those with $v_{neb} < 0$. Stars indicate SNe Ia occurring in pixels associated with SF ($NCR_{NUV} > 0$), circles indicate SNe Ia occurring in pixels with no association with SF ($NCR_{NUV} = 0$), and squares indicate SNe Ia with no NCR_{NUV} measurements. SN 2004eo, which only has a reported non-detection of Na in Pastorello et al. (2007) and for which we associate a typical error of 0.2 Å, is shown below the dotted line. In this figure, SNe Ia with $v_{neb} < 0$ appear clustered at relatively low EW values, with three exceptions at high EWs, whereas $v_{neb} \geqslant 0$ SNe Ia tend to have higher EWs in general. This suggests that the intervening CSM absorbs more light opposite to the direction of where the ignition occurs.

The fact that some SNe Ia show high EWs and $v_{neb} < 0$ (3 out of 14) is expected, since in some cases the EWs will
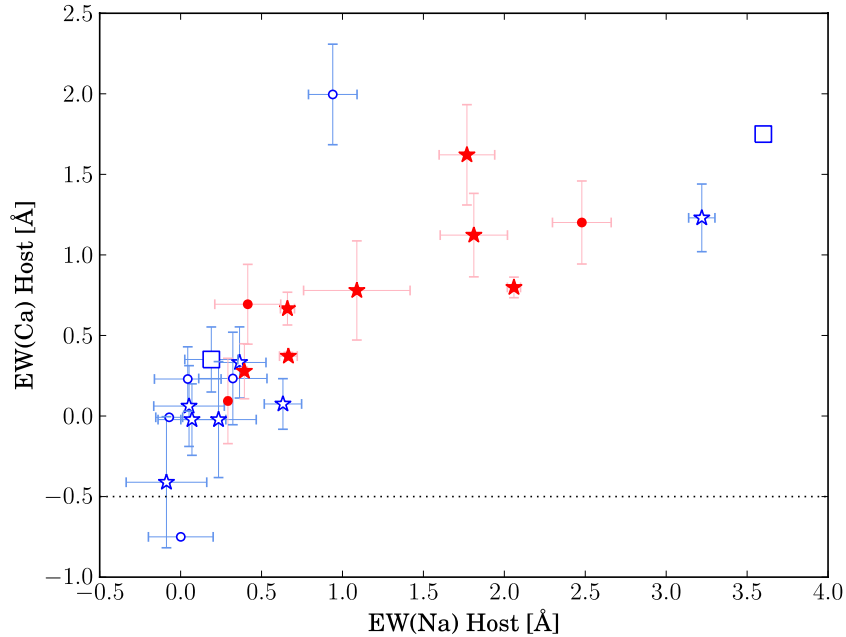
Figure 2. Equivalent widths of Ca vs. Na lines due to intervening material at the redshift of the SN host galaxies. We show SNe Ia with $v_{neb} \geqslant 0$ as red filled symbols, and those with $v_{neb} < 0$ as blue open symbols. SNe Ia occurring in pixels with $NCR_{NUV} > 0$ are shown as stars, those with $NCR_{NUV} = 0$ are shown as circles, and those with no measured NCR_{NUV} are shown as squares. The three SNe Ia with $v_{neb} < 0$ at high EWs are SN 1986G (open blue square), SN 2006dd (open blue star), and SN 2009dc (open blue circle). SN 2004eo, for which we only have EW(Na) information, is shown below the dotted line.
(A color version of this figure is available in the online journal.)

Table 2
K-S Test for Na and Ca Lines

K-S Test	$E(B-V)^{SNooPy}$	$(B-V)^{SiFTO}_{B_{max}}$	MW Na	Host Na	MW Ca	Host Ca
p-value	0.006	0.002	0.268	0.013	0.402	0.030

Note. The null hypothesis is that SNe Ia with negative and positive v_{neb} have the same distribution of colors or EWs for a given line due to the Milky Way (MW) or intervening material at the distance of the SNe.

Table 3
K-S Tests for Environmental Differences between SNe Ia
with Negative and Positive v_{neb}

K-S Test	Morphological Type	Galaxy Inclination	NCR_{NUV}	$NCR_{H\alpha}$
p-value	0.133	0.390	0.768	0.944

Note. The null hypothesis is that the distribution of global (morphological type and inclination) and local (NCR_{NUV} and $NCR_{H\alpha}$) host properties is the same.

be due to host galaxy material and not CSM absorption. Even if their high EWs are due to CSM, our K-S tests rule out that these exceptions are significant. In particular, SN 1986G and SN 2006dd appear to be located behind prominent dust lanes of their host galaxies and SN 2006dd has the second highest NCR_{NUV} statistic in our sample (0.827), implying a possible association with SF. However, SN 2006dd and SN 2009dc have been suggested to show some signs of CSM based on their Na line evolution (Stritzinger et al. 2010) and light curve shape (Taubenberger et al. 2011), hence we cannot rule out that their high EWs are due to CSM.

Most SNe Ia with $v_{neb} \geqslant 0$ in Figure 2 have some degree of association with SF ($NCR_{NUV} > 0$), which could be associated with higher EWs due to non-CSM in the line of sight. However, only 2 out of 10 SNe Ia with $v_{neb} \geqslant 0$ are strongly associated with SF ($NCR_{NUV} \geqslant 0.5$), whereas 4 out of 15 SNe with $v_{neb} < 0$ are strongly associated with SF. This suggests that

higher EWs in our sample are not primarily due to host galaxy non-CSM, which is consistent with the excess of blueshifted Na lines found by Sternberg et al. (2011), and which is supported by the high p-values for the NCR_{NUV} and $NCR_{H\alpha}$ K-S tests in Table 3. It could also be argued that NCR statistics are only a measure of relative SF within galaxies. To account for this, we have removed early-type galaxies from our sample and repeated the K-S tests from Table 2, obtaining significantly low p-values of 0.022 and 0.018 for the distribution of EW(Na) and EW(Ca), respectively.

4. DISCUSSION AND CONCLUSIONS

Our main conclusion is that the distribution of EWs from narrow blended Na and Ca lines differs significantly between SNe Ia with negative and positive v_{neb}. Because the sign of v_{neb} should be purely geometrical, it should not correlate with any host galaxy or average SN properties. This suggests that part of the lines are formed by CSM ejected by the progenitor before explosion, which is found asymmetrically distributed after explosion. The differences in color found for SNe Ia with different v_{neb} (Maeda et al. 2011), which we confirm using SNooPy and SiFTO light curve fitting, should be explained in part by extinction due to an asymmetric distribution of CSM, and not by different ejecta temperatures with viewing angle alone.

There are two possibilities to explain this result: (1) the CSM material is asymmetrically ejected from the system *before*

explosion and is aligned with the side of the ejecta where ignition occurs or (2) the CSM material is initially spherically symmetric and is affected by an asymmetric distortion *after* explosion, which is stronger on the side where ignition occurs.

One possible physical process that could break the symmetry of the WD and have an effect on both the direction of ignition and the distribution of CSM is rotation. However, rotation should produce cylindrically symmetric systems, where positive or negative v_{neb} should lead to the same average CSM properties in the line of sight. Another possibility is the gravitational field of a companion star, but the typical velocity offsets found for the absorbing material in Sternberg et al. (2011) imply that the material was ejected at a time before explosion much longer than the expected orbital period of the progenitor systems, again producing some cylindrical symmetry in average.

Thus, we conclude that only (2) is possible to explain our results. One way to produce an asymmetric distribution of dust, EW(Na), and EW(Ca) is to have an asymmetric ionizing field *after* explosion. This would destroy most of the dust and ionize Na and Ca in the direction where ignition occurs. A comparison with pre-explosion images of the core-collapse SN 2012aw (Fraser et al. 2012) supports the idea of dramatic changes in extinction after explosion. The fact that the correlations are found to be stronger for dust (colors) than for EW(Na) and EW(Ca) is suggestive, since they are in ascending order of ionization potential. One problem with this interpretation could be the constraints in radio and X-ray for CSM–ejecta interactions. This would be solved if the material were placed far enough from the ejecta, and only in some cases allowed the ejecta to interact with the CSM, as was seen in SN 2002ic, SN 2006X, and 2007le, or if the measured EWs are due to saturated lines in low-mass, clumpy CSM with a wide distribution of velocities.

Our results provide hints about the explosion asymmetry and CSM properties of SN Ia progenitors. If a larger sample confirms that most SNe Ia with $v_{neb} \geqslant 0$ have high EWs of Na and Ca absorption lines, then the majority of progenitors should contain significant CSM. If this is the case, then most SNe Ia with $v_{neb} < 0$ should have more strongly ionizing fields (higher energy photons) after explosion, either during shock breakout, or afterward if more radioactive material is exposed in the ignition side of the explosion.

Finally, significant CSM is consistent with some M_{Ch}–SD or slow DD scenarios (e.g., Fryer et al. 2010) and not with violent DD scenarios. However, in our interpretation, it is difficult to explain the SNe Ia with $v_{neb} \geqslant 0$ and low EWs, which may suggest that multiple progenitor scenarios are at work.

REFERENCES

Barbon, R., Buondí, V., Cappellaro, E., & Turatto, M. 1999, A&AS, 139, 531
Benetti, S., Cappellaro, E., Turatto, M., et al. 2006, ApJ, 653, L129
Blondin, S., Matheson, T., Kirshner, R. P., et al. 2012, AJ, 143, 126
Blondin, S., Prieto, J. L., Patat, F., et al. 2009, ApJ, 693, 207
Bloom, J. S., Kasen, D., Shen, K. J., et al. 2012, ApJ, 744, L17
Branch, D., Garnavich, P., Matheson, T., et al. 2003, AJ, 126, 1489
Brown, P. J., Dawson, K. S., de Pasquale, M., et al. 2012, ApJ, 753, 22
Burns, C. R., Stritzinger, M., Phillips, M. M., et al. 2011, AJ, 141, 19
Cartier, R., Förster, F., Coppi, P., et al. 2011, A&A, 534, L15
Chugai, N. N. 2008, Astron. Lett., 34, 389
Conley, A., Sullivan, M., Hsiao, E. Y., et al. 2008, ApJ, 681, 482
Folatelli, G., Phillips, M. M., Burns, C. R., et al. 2010, AJ, 139, 120
Foley, R. J. 2012, ApJ, 748, 127
Foley, R. J., Simon, J. D., Burns, C. R., et al. 2012, ApJ, 752, 101
Fraser, M., Maund, J. R., Smartt, S. J., et al. 2012, arXiv:1204.1523
Fryer, C. L., Ruiter, A. J., Belczynski, K., et al. 2010, ApJ, 725, 296
Gerardy, C. L., Meikle, W. P. S., Kotak, R., et al. 2007, ApJ, 661, 995
Goobar, A. 2008, ApJ, 686, L103
Hamuy, M., Phillips, M. M., Suntzeff, N. B., et al. 1996, AJ, 112, 2408
Hamuy, M., Phillips, M. M., Suntzeff, N. B., et al. 2003, Nature, 424, 651
Hillebrandt, W., & Niemeyer, J. C. 2000, ARA&A, 38, 191
Höflich, P., Gerardy, C. L., Nomoto, K., et al. 2004, ApJ, 617, 1258
Horesh, A., Kulkarni, S. R., Fox, D. B., et al. 2012, ApJ, 746, 21
James, P. A., & Anderson, J. P. 2006, A&A, 453, 57
Jha, S., Garnavich, P. M., Kirshner, R. P., et al. 1999, ApJS, 125, 73
Khokhlov, A. M. 1991, A&A, 245, L25
Maeda, K., Benetti, S., Stritzinger, M., et al. 2010, Nature, 486, 82
Maeda, K., Leloudas, G., Taubenberger, S., et al. 2011, MNRAS, 413, 3075
Matheson, T., Kirshner, R. P., Challis, P., et al. 2008, AJ, 135, 1598
Nomoto, K., Thielemann, F.-K., & Yokoi, K. 1984, ApJ, 286, 644
Nonaka, A., Aspden, A. J., Zingale, M., et al. 2012, ApJ, 745, 73
Nugent, P. E., Sullivan, M., Cenko, S. B., et al. 2011, Nature, 480, 344
Pakmor, R., Kromer, M., Taubenberger, S., et al. 2012, ApJ, 747, L10
Pastorello, A., Mazzali, P. A., Pignata, G., et al. 2007, MNRAS, 377, 1531
Patat, F., Chandra, P., Chevalier, R., et al. 2007, Science, 317, 924
Perlmutter, S., Aldering, G., Goldhaber, G., et al. 1999, ApJ, 517, 565
Phillips, M. M. 1993, ApJ, 413, L105
Phillips, M. M., Phillips, A. C., Heathcote, S. R., et al. 1987, PASP, 99, 592
Riess, A. G., Filippenko, A. V., Challis, P., et al. 1998, AJ, 116, 1009
Röpke, F. K., Kromer, M., Seitenzahl, I. R., et al. 2012, ApJ, 750, L19
Silverman, J. M., Ganeshalingam, M., Li, W., et al. 2011, MNRAS, 410, 585
Simon, J. D., Gal-Yam, A., Gnat, O., et al. 2009, ApJ, 702, 1157
Sternberg, A., Gal-Yam, A., Simon, J. D., et al. 2011, Science, 333, 856
Stritzinger, M., Burns, C. R., Phillips, M. M., et al. 2010, AJ, 140, 2036
Taubenberger, S., Benetti, S., Childress, M., et al. 2011, MNRAS, 412, 2735
Vernet, J., Dekker, H., D'Odorico, S., et al. 2011, A&A, 536, A105
Wang, X., Li, W., Filippenko, A. V., et al. 2009, ApJ, 697, 380
Yaron, O., & Gal-Yam, A. 2012, arXiv:1204.1891